Journal of Archaeological Science: Reports 34 (2020) 102587

Contents lists available at ScienceDirect

Journal of Archaeological Science: Reports

journal homepage: www.elsevier.com/locate/jasrep

The effects of vertical position in the intertidal zone on the $\delta^{18}O$ and $\delta^{13}C$ composition of *Mytilus californianus* shell carbonate

Christopher S. Jazwa *, Christopher A. Wolfe, Elaine Y. Chu, Kyra E. Stull

Department of Anthropology, University of Nevada, Reno, NV 89557, United States

ARTICLE INFO

Keywords:
Stable isotope analysis
Paleoecology
Seasonality
Coastal archaeology
California
Channel Islands
Experimental archaeology

ABSTRACT

Stable oxygen ($\delta^{18}O$) isotopic measurements of marine shell carbonate are useful proxies for reconstructing past marine conditions on time scales that are relevant for archaeological interpretations. This includes long-term changes in sea surface temperature (SST) and estimates of the season of harvest of shells, with implications for site seasonality and mobility. As these studies are applied with more frequency, it becomes important to look at relevant details of the ecology of the species that is being tested. We conduct an experimental study on *Mytilus californianus* (California mussel) shells from a piling on the pier at Bechers Bay on Santa Rosa Island, California to assess the effects of vertical position in the water column on shell length, $\delta^{18}O$, and stable carbon ($\delta^{13}C$) isotopic measurements. Shell length has the most substantial relationship of the three. It increases with depth and therefore time spent submerged, up to a maximum point. This difference can be as much as 45%. $\delta^{18}O$ has a statistically significant negative trend with depth, which can result in an offset of 1.8 °C in extreme cases. $\delta^{13}C$ does not have a clear pattern with depth. This study indicates that while stable isotopic measurements of California mussel shells can still be used in paleoenvironmental reconstructions, it is necessary to be aware of additional error sources in estimates of annual SST ranges and ideally, interpretations of season of harvest of an individual shell should be made independently from other shells.

1. Introduction

Conducting stable isotopic measurements on marine mollusk shell carbonate is a useful method for reconstructing past environmental conditions in coastal environments. Additionally, when the shells that are tested are derived from cultural deposits at archaeological sites, those conditions can be directly attributed to the chronology of human activities there. This reduces the need to reconcile time scales between natural paleoenvironmental proxies and cultural activities. Furthermore, marine mollusk shells are often abundant at coastal midden sites, providing a wealth of opportunities to obtain data. Recent work pairing sclerochronology, the growth history of mollusk shells, with geochemical methods has led to successful advances in paleoenvironmental reconstruction (e.g., Andrus, 2011; West et al., 2018). Most of these studies rely on oxygen isotopic ($\delta^{18}O$) measurements as a proxy for sea surface temperature (SST). $\delta^{18}O$ values vary with the isotopic composition of seawater (including salinity) and water temperature (Urey, 1947; Wefer and Berger, 1987). Both variables can fluctuate seasonally in predictable ways, with the geographic context influencing their relative importance. In open-ocean contexts away from sources of freshwater input, fluctuations in salinity are much smaller than annual sea surface temperature change, making $\delta^{18}O$ an effective paleothermometer (Shackleton, 1973; Kennett and Voorhies, 1996; Jazwa et al., 2012, 2016; Jazwa, 2015; Butler et al., 2013; Hausmann et al., 2017; Prendergast and Schöne, 2017; Parker et al., 2017). Stable carbon isotope ratios ($\delta^{13}C$) are measured alongside $\delta^{18}O$ and can also be used to look at environmental shifts, including differential patterns in upwelling (Sadler et al., 2012; Graniero et al., 2017). Still, $\delta^{13}C$ is rarely applied without $\delta^{18}O$.

West et al. (2018) published a synthetic review of the current state of mollusks in paleoenvironmental reconstruction, including a discussion of sampling strategies and limitations to different approaches. Only some of these drawbacks can be determined retrospectively from the samples themselves. For example, recent studies have tested the effects of heating shells on the $\delta^{18}O$ and $\delta^{13}C$ values of shell carbonate (Milano et al., 2016; Müller et al., 2017; Jazwa and Jantz, 2019). They showed that high temperatures can alter the isotopic composition of shells, limiting their applicability for reliable environmental reconstruction in

* Corresponding author.
E-mail address: cjazwa@unr.edu (C.S. Jazwa).

https://doi.org/10.1016/j.jasrep.2020.102587
Received 5 May 2020; Received in revised form 31 August 2020; Accepted 2 September 2020
Available online 8 October 2020
2352-409X/

some conditions. This is particularly important in cases in which shells undergo visible alterations from high heat. Nevertheless, other conditions may affect the isotopic composition of mollusk shell carbonate in ways that may not be able to be observed in the shells either microscopically or macroscopically. For example, sessile intertidal species like mussels grow at an individual point that is fixed both horizontally (throughout the intertidal zone) and vertically (in the water column). The latter is especially relevant, because it regulates the amount of time the individual mollusk spends exposed to the air or under water, where it has access to nutrients (Coe and Fox, 1942; Harger, 1970; Suchanek, 1981; Thakar et al., 2017). This could promote different growth rates, which in turn leads to variation in isotopic composition of the shell carbonate drilled from the same distance to the terminal growth edge of different shells. Furthermore, because drilling samples necessarily combines powder from a range of deposition events, different shells may combine different date ranges, depending on the growth rate of the shell.

In this study, we assess the differences in shell size and stable isotopic values between California mussel (*Mytilus californianus*) shells collected at a single location on Santa Rosa Island, California, from controlled vertical positions. By consistently sampling each of the sets of shells from different depths, it is possible to determine the effects of vertical position in the intertidal zone and therefore how the amount of time spent underwater and exposed to the air affects the overall length of mussel shells and the $\delta^{18}O$ and $\delta^{13}C$ values at different sampling points on the shell. Unfortunately, it is not possible to determine from the archaeological record where within the range of locations in the intertidal zone an individual shell grew. Therefore, rather than attempting to correct for the depth of the shell, the goal is instead to assess whether any effects on the isotopic analysis conducted on the shell are large enough to alter paleoenvironmental interpretations or estimates of season of harvest for the shell. If variation in $\delta^{18}O$ values in particular can alter estimates of SST on the order of magnitude of the seasonal fluctuations, that species should only be useful if other information is available regarding where in the water column the shell was harvested. By conducting this experiment on *M. californianus*, we are testing the usefulness of this species for isotopic analysis, which will provide a framework for similar tests on other mollusks.

2. Background

2.1. Mytilus californianus ecology and growth

M. californianus has been the frequent subject of isotopic analysis from archaeological sites along the Pacific coast of North America primarily because of its abundance in shell middens (e.g., Coe and Fox, 1942, 1944; Glassow et al., 1994; Jones and Richman, 1995; Bettinger et al., 1997; Kennett, 1998; Jazwa et al., 2012, 2020, 2016; Jazwa, 2015; Jew et al., 2013, 2014; Thakar, 2014). Coastal sites on California's northern Channel Islands (NCI), for example, are typically dominated by this species of mussel and in many cases, it comprises over 50% of all dietary material by weight (e.g., Jazwa et al., 2016). *M. californianus* have been found in a wide geographic range, extending from the Aleutian Islands to Isla Socorro, Mexico, a small island to the south of the Baja California peninsula, although it is a dominant component of the intertidal region from British Columbia southward (Soot-Ryen, 1955; Suchanek, 1981). This species survives well in exposed coastal environments, primarily on rocky shorelines. Today, they also grow on artificial structures like pilings for piers, oil platforms, and other structures (Harger, 1970; Suchanek, 1981). *M. californianus* can survive at a range of depths within the intertidal and subtidal, but it is most abundant in the intertidal band. Suchanek (1978) noted a range from 1.3 m to 2.9 m above mean lowest low water on the Washington coast, but Paine (1976) has observed them as deep as 30 m. Within the intertidal range, *M. californianus* is the dominant species, but a wide variety of other sessile or mobile species live among them. On the NCI, the most common species that live among mussel beds include *Tegula funebralis, Pollicipes polymerus, Haliotis cracherodii, Ischnochiton conspicuus, Balanus* spp., and a variety of small gastropods.

Mussel growth rate is influenced by several environmental factors, including water temperature, food supply, sex, and age (Coe and Fox, 1942, 1944). *M. californianus* has the potential to spawn throughout the year, promoting communities with a wide range of growth stages (Suchanek, 1978, 1981). The fastest growth rates are typically observed in the smallest individuals, and they slow with size and age. In a study of annual growth rates among *M. californianus*, Coe and Fox (1942) observed average annual growth for small (starting at 10 mm) individuals was 60 mm. Individuals starting between 10 and 40 mm had an average annual growth ranging between 40 and 60 mm, and individuals starting between 50 and 70 mm had an average annual growth between 32 and 36 mm. Larger individuals had progressively slower growth rates, with 110 mm individuals increasing only 14 mm on average in a year.

Growth also varies throughout the year. The higher average growth rates were during the colder water months from November to May, although there was considerable variation and Coe and Fox (1942) caution that this may not be applicable to regions further north than southern California. This may be related to seasonal differences in upwelling, which promotes greater productivity and therefore increased growth. In their study, Coe and Fox (1942) kept their experimental populations below the intertidal zone, indicating that it is not necessary for mussels to be exposed to the surf for survival. Instead, they found that mussels benefit from periodic exposure only as a protection against sea stars, fishes, crustaceans, and other predators, which determine the lower boundary of the mussel beds. They did, however, observe that the highest levels of mussels (i.e., most time exposed to air) appear to grow slower than deeper individuals. A study by Thakar et al. (2017) from nearby Santa Cruz Island, California, indicated that growth rate for California mussels increases with depth into the lower-intertidal and subtical zones. Mussel growth can be intermittent, with periods of rapid and delayed growth that can be influenced by temperature, decreases in food supply, storms, and exposure to air between tides (Coe and Fox, 1942).

2.2. Stable isotopic analysis of M. Californianus shell carbonate

Like many paleoenvironmental proxies, *Mytilus californianus* has both beneficial characteristics and limitations. The biggest advantage is its abundance in archaeological contexts because there are relatively few locations on the Pacific Coast in which most shell middens are not dominated by the species. Furthermore, growth bands are deposited in such a way that carbonate can be sampled to represent a range of time periods along the growth axis. It is sufficiently fast growing that fine-scale sampling is possible to detect isotopic variation on the scale of seasons or possibly even shorter time scales (West et al., 2018; Coe and Fox, 1942; Jew et al., 2014). An additional benefit is that the outer shell is calcite rather than aragonite. Calcite is less likely to have its stable carbon and oxygen isotopic ratios altered when the shell is subjected to heat (Andrus and Crowe, 2002; Milano et al., 2016; Müller et al., 2017; Jazwa and Jantz, 2019) and we are drilling only the outer, calcite layer of the shell. On the other hand, *M. californianus* is limited as a proxy because there is a high potential for intershell variability in the isotopic profile. Because growth can be intermittent, which can include periods of rapid growth and disturbance (Coe and Fox, 1942; Suchanek, 1981), this can lead to difficulty associating individual samples with specific deposition time, leading to errors in water temperature estimates. Furthermore, because powder is often drilled using a drill bit with a non-zero diameter (often 0.5–0.8 mm), it includes material from a time scale of several days or even weeks. Differences in growth rates even between mussels of the same age or starting size can also lead to variability in the isotopic profile and patterns in estimated SST. Furthermore, patterns in local upwelling can also affect the isotopic composition of shells (Flores, 2017). It is for these reasons that many archaeologists use multiple shells

to reconstruct annual patterns in $\delta^{18}O$ (e.g., Kennett, 1998). When estimating seasonal patterns of mussel harvesting at a site, there is consensus that more than two samples must be collected per shell, although the exact number of samples to best mitigate the effects of this variability while minimizing sampling costs is still in development (e.g., Jew et al., 2013, 2014; Thakar, 2014; Jazwa, 2015). Sclerochronological methods have also proven effective for distinguishing growth bands on individual shells of other species to maximize precision, and this could be promising for *M. californianus* as well (e.g., Andrus, 2011; West et al., 2018; Thomas, 2015; Butler et al., 2013; Butler and Schöne, 2017; Prendergast et al., 2018).

Our sampling location is from a piling on the southern side of Bechers Pier, the main point of access to Santa Rosa Island, the second largest of the NCI and a part of Channel Islands National Park (Fig. 1). This location is offshore from the mainland, with no major freshwater inputs to the system. Based on ocean water samples collected by CSJ at increments of three months or less from August 2015 to May 2019, it appears that variation in the $\delta^{18}O$ of ambient seawater throughout the year is relatively small (Table 1). The $\delta^{18}O$ of ambient seawater was measured on a Picarro L2130-I spectroscopic isotope water analyzer at the Nevada Stable Isotope Laboratory at the University of Nevada, Reno (UNR) and has a measurement error of 0.1‰. The average $\delta^{18}O$ value for the pier is −0.3‰, with a median of −0.4‰. All but 3 of the 18 values are between −0.3‰ and −0.4‰, and only a single value is not between −0.1‰ and −0.4‰. Without that outlier, which may be a faulty measurement or from a contaminated sample, the standard deviation on these measurements is only 0.1‰. This would indicate that fluctuation in SST is the dominant source of variation in the $\delta^{18}O$ signature.

SST at the time of carbonate deposition can be estimated using the equation for calcite established by Horibe and Oba (1972):

$$t^{\circ}C = 17.04 - 4.34(\delta c - \delta w) + 0.16(\delta c - \delta w)^2 \quad (1)$$

Table 1
$\delta^{18}O$ and δD measurements of seawater presented relative to VSMOW. Samples were collected from the mussel sampling location at Bechers Pier at intervals of three months or less between August 2015 and May 2019. The January 2016 sample was collected by Cause Hanna and the January 2018 sample was collected by Geoff Dilly, both from California State University, Channel Islands.

Date	$\delta^{18}O_{VSMOW}$ (‰)	δD_{VSMOW} (‰)
6 August 2015	−0.6	−4
1 November 2015	−0.3	−4
17 January 2016	−0.5	−3
21 March 2016	−0.6	−4
11 May 2016	−0.5	−4
8 August 2016	−0.5	−4
15 November 2016	−0.4	−4
24 March 2017	−0.2	−2
23 May 2017	−0.3	−3
6 August 2017*	−0.4	−3
24 September 2017	−0.4	−3
6 January 2018	−0.4	−3
21 March 2018	−0.5	−4
22 May 2018	−0.3	−3
21 August, 18**	0.4	−1
19 October 2018	−0.1	−2
15 March 2019	−0.3	−3
24 May 2019	−0.4	−3
Average	−0.4	−3.2
Standard Deviation	0.1	0.6
Median	−0.4	−3.3

*Water sample collected concurrently with M. californianus shells.
**This sample is a likely outlier and not included in the summary statistics.

This was modified from the original equation in Epstein et al. (1953), in which δc is the measured $\delta^{18}O$ value from the sample and δc is the $\delta^{18}O$ value of ambient seawater. Using an example value for δc of 0‰, a variation in ambient seawater between −0.3‰ and −0.6‰ would yield

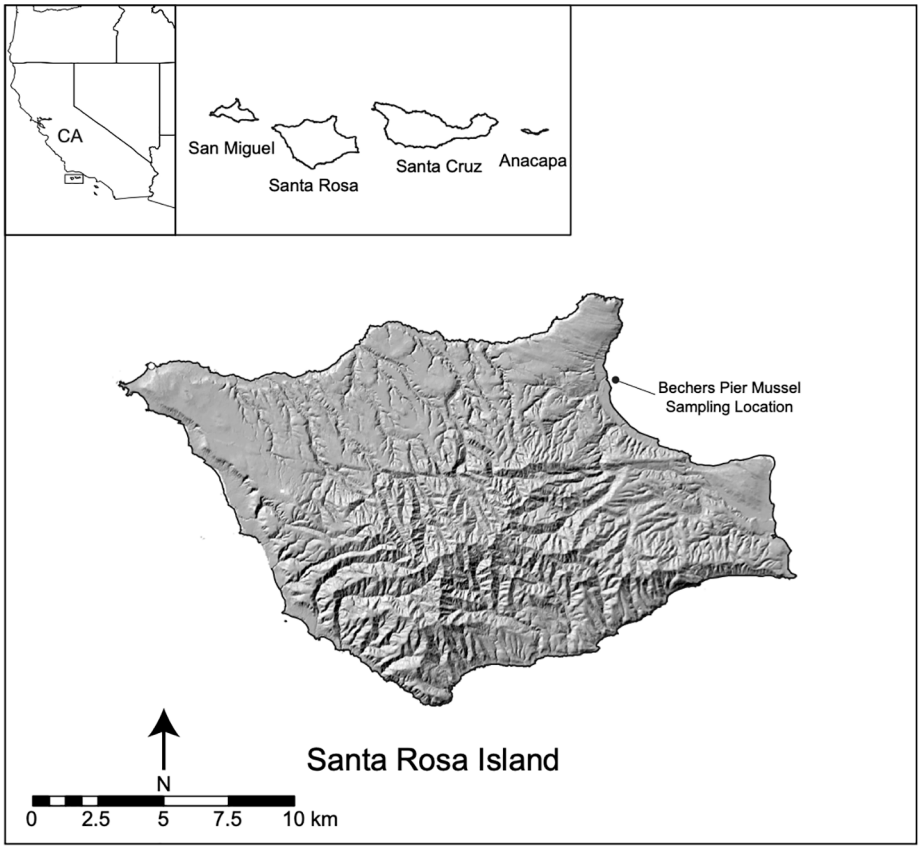

Fig. 1. Santa Rosa Island, California, with the Bechers Pier mussel sampling location indicated.

a difference in temperature estimates of 1.35 °C, and a variation between −0.3‰ and −0.4‰ would yield a difference of 0.45 °C. Even the more extreme difference is much less than seasonal variation in water temperatures, which can be 10 °C or more. Averaged water temperature values from 1981 to 1992 measured off the coast of Santa Rosa Island by J. Engle and smoothed with a 15-day running average indicate a modern annual range of average daily water temperatures between 13 °C and 18 °C, although daily measurements ranged from 11 °C and 21 °C (Jazwa et al., 2015).

A frequent application of $\delta^{18}O$ measurements on shell carbonate is to make inferences about the season of harvest of that species, with inferences for season of site occupation (e.g., Shackleton, 1973; Glassow et al., 1994; Kennett and Voorhies, 1996; Colonese et al., 2011; Thompson and Andrus, 2011; Eerkens et al., 2014; Gutiérrez-Zugasti et al., 2017; Loftus et al., 2019; Branscombe et al., 2020). However, these analyses must be considered in the context of the overall archaeological record at a site. If some species or groups of species (i.e., shellfish) are not major contributors to the faunal assemblage from a site, they may not be reliable indicators of overall site seasonality. Instead, they may only reflect the season of collection of that species, which may not be the entire range of time the site is occupied. For example, in most cases on the NCI, *M. californianus* is the dominant contributor, with some notable exceptions including large Late Period (650–168 cal BP) villages in which fish constitutes the dominant contributor to diet and shellfish may be only supplementary (e.g., Jazwa et al., 2020). In addition to its near ubiquity on the Pacific Coast and beneficial characteristics for paleotemperature reconstructions, *M. californianus* meets the criteria established by Shackleton (1973) as an effective proxy to model the seasonality of site occupation.

3. Methods

3.1. Shell harvesting and data collection

All shell samples were harvested from the south side of Bechers Pier (Fig. 2) on August 6, 2017 by CSJ and Kevin Smith. We chose a piling that does not come into contact with any boats while they are being loaded or unloaded to minimize the potential that the sample would be biased by shells being routinely dislodged. We collected the shells in the afternoon within an hour of the 0.65 m low tide (3:25 PM). A spring low tide occurred at 4:36 AM on August 7 (-0.11 m) and spring high tide occurred at 10:09 PM on August 7 (1.72 m). The $\delta^{18}O$ of ambient seawater at the time of collection was measured at −0.4‰ (Table 1). The band of mussels on the piling of the pier sampled for this test was approximately 100 cm thick (Fig. 2). Small barnacles, which can survive with even less frequent submergence, extend above the top of the mussel colony, but the top of the mussel growth range exists at a distinct boundary. All samples were harvested using the plucking method (Jones and Richman, 1995) from arbitrarily defined 10 cm levels, starting at the top of the mussels. From each 10 cm level, we collected between 6 and 9 shells indiscriminately of shell size. Therefore, the shells collected from each level are not biased by an intentional selection for shells of any particular size. We processed all of the mussels on site using a dull metal knife. First, we scraped off barnacles. Then, we pried mussels open and scraped the meat out. After washing the shells in fresh water at the National Park Service housing unit, we left them to dry overnight.

Fig. 2. Bechers Pier at a spring low tide, with mussels visible on the pilings. The sampled location is indicated with the top and bottom of the cluster of mussels.

We cleaned and drilled the *M. californianus* shells at the Human Paleoecology and Archaeometry Laboratory at UNR. Prior to chemical processing, all sample lengths were measured from the umbo to the furthest point on the outer shell edge using calipers. We then sonicated the shells in deionized water for 30 min. We subjected the shells to a HCl etch at 70 °C to expedite the reaction. The volume and concentration of HCl was calculated to remove 10% of the outside shell carbonate by weight. Acid etching reduces the chance of contamination from barnacle shells that were removed manually but may have left residual carbonate. After drying the shells, the outer organic periostracum was abraded off of each shell in a 1 cm wide channel along the growth axis using the side of a 0.8 mm drill bit on a Dremel tool at low speed. We obtained five samples from each shell, drilling only the outer prismatic layer to ensure that the powder was calcite and avoid the inner, aragonite layers that are not deposited in bands that reflect changes through time (Dodd, 1964). For each shell, samples were drilled from the outer edge of the shell (terminal growth band), 1 mm, 2 mm, and 3 mm from the edge, and in a profile extending from 0 to 3 mm from the edge. The 0–3 mm profile represents an average of all of the environmental conditions over the final 3 mm of deposition. For mid-life shells, this may represent 1–2 months of growth (Coe and Fox, 1942). All drilling was done at low speed to minimize isotopic fractionation. We chose a relatively large drill bit with an 0.8 mm diameter (rather than 0.5 mm, for example) to include a larger range of carbonate deposits in each sample and minimize error from drilling shells in slightly different locations. All powder was folded into small envelopes made from weigh paper and submitted to the stable isotope laboratory in the Department of Sediment and Isotope Geology at Ruhr-Universität Bochum in Germany for analysis. Measurements were conducted on a ThermoFisher Scientific MAT 253 IRMS coupled with a GasBench II following the procedure given in Breitenbach and Bernasconi (2011). Long-term uncertainties on this instrument are 0.16‰ for both $\delta^{13}C$ and $\delta^{18}O$.

3.2. Statistical methods

We applied statistical analyses to determine whether shell length, $\delta^{13}C$, and $\delta^{18}O$ vary significantly with vertical position in the water column, and if so, the magnitude of that difference. Because of small sample sizes across groups, unequal variances across shell depth and/or water depth, and possible outliers in shell size or isotopic values, we applied non-parametric methods that are not subject to the distributional assumptions that may bias the true effect of vertical position (Button et al., 2013; Colquhoun, 2017). The Kruskal-Wallis test by ranks (K-W) is a non-parametric method to test the hypothesis that samples of independent data may be from the same distribution (population) and therefore, contain similar sample median values and mean ranks (Kruskal and Wallis, 1952). The K-W test is an extension of the Mann-Whitney U Test towards multiple groups and is the non-parametric equivalent of a one-way analysis of variance (ANOVA). Statistically, K-

W results ($p \leq 0.05$[1]) reveal that at least one of the multiple comparisons were significant, but the results do not identify the pairwise comparison (s) that demonstrate significance. Subsequently, if K-W test results were statistically significant, the post-hoc Dunn's Test of Multiple Comparisons using Rank Sums was used to identify such statistically significant pairwise differences occur. Iterating throughout the entire sample, Dunn's test computes multiple pairwise comparisons among each group to test for differences in median isotopic composition (Dunn, 1964). The p-values had a Holm's adjustment to account for the number of statistical tests to ensure there was not an increased likelihood of a Type I error (Holm, 1979). Because of the adjustment associated with the Dunn's Test, we reject the null hypothesis if $p <= \alpha/2$ (if $\alpha = 0.05$, then we reject H_0 if $p <= 0.025$).

The above-described analyses were run separately for $\delta^{13}C$ and $\delta^{18}O$. Each set of these analyses was also run separately for the 0–3 mm profile values by water column depth and by location on the growth axis of the shell (i.e., 0, 1, 2, or 3 mm) by water column depth. All analyses were completed in the R programming environment (R Core Team, 2018). Additional packages include *ggplot2* (Wickham, 2016) for visualizations and *dunn.test* (Dinno, 2017) for the post-hoc Dunn's test.

4. Results

4.1. Shell size

Overall, there are clear patterns in shell length in relation to the vertical position in the water column (Table 2; Fig. 3). The uppermost shells are the smallest, with the average shell lengths in all three depth levels from 0 to 30 cm less than 70 mm. These shells spend the most time out of the water and exposed to air, which slows their growth since it prevents access to nutrients in the water column. The uppermost levels may spend entire days out of the water during neap tides. Overall, there is a general pattern toward increasing shell length from 0 to 10 cm (60.1 mm average length), up to 50–60 cm (87.4 mm) and 60–70 cm (87.0 mm), before a decrease to the deepest levels, 80–90 cm and 90–100 cm (72.4 mm at both levels). This pattern indicates that there may be a peak vertical depth range in the intertidal zone for *M. californianus* shell length. In this experiment, this depth is between 50 and 80 cm below the top of the mussel growth range. In all three of the levels in that range, the average mussel lengths are greater than 80 mm.

4.2. $\delta^{18}O$ variation with depth

Stable oxygen isotopic measurements reflect statistically significant patterns from the top to the bottom of the mussel bed (Tables 3–5). We first analyzed the values for $\delta^{18}O$ from 0 to 3 mm profiles. We chose these samples to try to minimize errors associated with any intershell differences in where point samples were drilled, either as a result of small sampling differences or differences in growth rates between individual shells. Visually, there appears to be a negative trend in $\delta^{18}O$ values as water depth increases, with especially high variability at the shallowest depths (Fig. 4a). K-W test results suggest a statistically significant difference between depths ($X^2 = 24.73$, df = 9, p-value = 0.004). However, the post-hoc Dunn's test indicates that the significant differences were the pairwise comparisons between the smallest and greatest depths (Table 4). Specifically, the significant differences were between 0 and 10 cm and 80–90 cm (z-statistic = 4.08, p-value = 0.001) and between 20 and 30 cm and 80–90 cm (z-statistic = 3.30, p-value = 0.021). This may be a product of the high variability of $\delta^{18}O$ within levels and relatively small sample size. We also assessed the differences in $\delta^{18}O$ between different depths for individually sampled points, 0 mm, 1 mm, 2 mm, and 3 mm from the terminal growth band (Fig. 4b). These values are highly variable, and variability increases with water depth. While there appears to be a decrease in $\delta^{18}O$ with depth for each of the locations on the shell individually, statistical analyses do not yield any significant differences.

We can assume independence between the measurements on an individual shell because they each represent a distinct point in time and each sample on a shell does not influence any of the others (or aggregate of several days or weeks). Furthermore, because each mussel remains at the same depth once it attaches to the substrate early in life, measurements at each point along the growth axis for each shell should be similarly affected by depth. This allows us to increase the sample size for the analysis by combining all of the previous comparisons for each of the individual points along the growth axis of the shells into an aggregated data set (i.e., 0 mm only compared to 0 mm values, 1 mm only compared to 1 mm values, etc.) to test the overall differences in $\delta^{18}O$ along the water column. The result employs the same pairwise comparisons as the previous method, but quadruples the number of data points in the analysis. In this context, there appears to be a slight negative trend in $\delta^{18}O$ values (Table 3). The K-W test indicates significant differences in measurements of some depth pairs ($X^2 = 70.721$, df = 9, p-value = 0.000) and the Dunn's test reveals the surface and bottom levels significantly differ from each other (z-statistic = 4.27, p-value = 0.000; Table 5). The magnitude of this difference is small but not negligible, with the difference of the means of $\delta^{18}O$ values from 90 to 100 mm lower than those from 0 to 10 cm by 0.42‰.

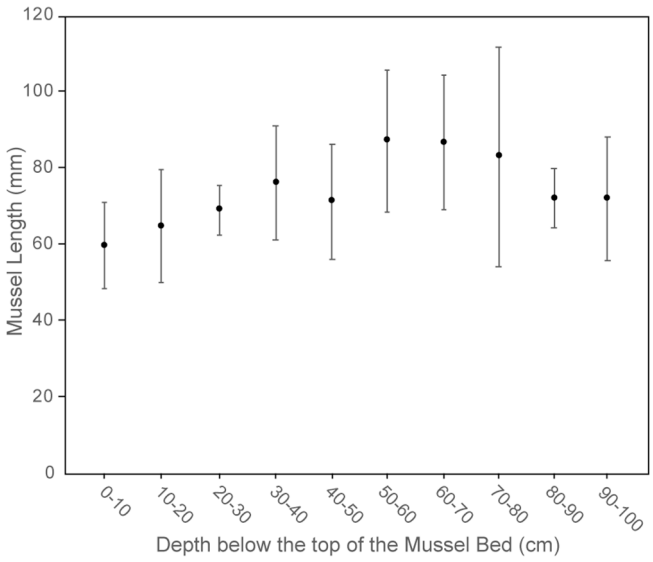

Fig. 3. Average mussel length by depth. Lines represent standard deviations.

Table 2
Average lengths of mussels collected from each 10 cm vertical increment on the piling, along with standard deviations.

Depth	Average (mm)	Median (mm)	Standard Deviation (mm)
0–10 cm	60.1	61.1	11.3
10–20 cm	65.1	71.0	14.7
20–30 cm	69.4	68.5	6.5
30–40 cm	76.5	77.8	14.9
40–50 cm	71.7	73.1	15.0
50–60 cm	87.4	85.1	18.5
60–70 cm	87.0	81.9	17.6
70–80 cm	83.3	100.5	28.6
80–90 cm	72.4	72.3	7.8
90–100 cm	72.4	73.6	16.0

[1] This value for significance was chosen by convention. None of the test results in this study are near this boundary, so interpretations of significance are not influenced by this decision.

Table 3
Average $\delta^{18}O$ and $\delta^{13}C$ measurements for all sample points between shells at each 10 cm vertical increment, along with standard deviations.

	$\delta^{13}C$								$\delta^{18}O$							
	0 mm		1 mm		2 mm		3 mm	0–3 mm Profile	0 mm		1 mm		2 mm		3 mm	0–3 mm Profile
Depth	Avg	StDev	Avg	StDev	Avg	StDev	Avg	StDev	Avg	StDev	Avg	StDev	Avg	StDev	Avg	StDev	Avg	StDev	Avg	StDev
0–10 cm	−0.20	0.22	−0.29	0.18	−0.51	0.30	−0.41	0.26	−0.48	0.19	−0.25	0.27	−0.21	0.22	0.09	0.66	0.33	0.41	0.17	0.37
10–20 cm	−0.15	0.26	−0.26	0.19	−0.43	0.29	−0.47	0.26	−0.44	0.23	−0.35	0.30	−0.34	0.16	−0.26	0.53	−0.19	0.37	−0.19	0.43
20–30 cm	−0.09	0.28	−0.28	0.41	−0.35	0.38	−0.57	0.26	−0.38	0.23	−0.22	0.16	−0.18	0.31	−0.20	0.44	−0.19	0.27	−0.03	0.24
30–40 cm	−0.18	0.35	−0.27	0.31	−0.26	0.17	−0.53	0.24	−0.29	0.19	−0.42	0.26	−0.28	0.26	−0.29	0.26	−0.21	0.39	−0.17	0.35
40–50 cm	−0.20	0.24	−0.28	0.28	−0.40	0.26	−0.48	0.31	−0.44	0.27	−0.38	0.20	−0.23	0.15	−0.31	0.24	−0.44	0.22	−0.36	0.20
50–60 cm	−0.06	0.21	−0.15	0.21	−0.37	0.32	−0.40	0.12	−0.39	0.21	−0.26	0.22	−0.36	0.27	−0.41	0.11	−0.25	0.46	−0.30	0.19
60–70 cm	−0.34	0.34	−0.32	0.19	−0.48	0.29	−0.51	0.36	−0.41	0.28	−0.54	0.11	−0.36	0.18	−0.48	0.13	−0.34	0.20	−0.35	0.16
70–80 cm	−0.46	0.15	−0.36	0.17	−0.56	0.24	−0.76	0.37	−0.57	0.13	−0.62	0.22	−0.40	0.22	−0.45	0.25	−0.43	0.23	−0.35	0.21
80–90 cm	−0.33	0.21	−0.44	0.21	−0.54	0.20	−0.75	0.35	−0.49	0.26	−0.61	0.24	−0.65	0.19	−0.74	0.18	−0.63	0.24	−0.58	0.27
90–100 cm	−0.33	0.25	−0.45	0.14	−0.68	0.14	−0.75	0.25	−0.65	0.16	−0.53	0.26	−0.40	0.28	−0.53	0.37	−0.52	0.38	−0.46	0.37

A second alternative to increase sample size is to combine measurements from shells to 20 cm vertical levels (i.e., 0–20 cm, 20–40 cm, 40–60 cm, 60–80 cm, 80–100 cm; Fig. 4c). Here, we focus on the measurements taken at the shell edge (0 mm) and 1 mm from the edge, which are the least likely to have differences between levels conflated with variability resulting from differences in shell growth rate. For those samples collected from the terminal growth band, there are significant differences in $\delta^{18}O$ between each of the three upper vertical levels and the two vertical levels. The largest difference between mean values is a decrease with depth of 0.26‰, which occurs between 20 and 40 cm and 60–80 cm (z-statistic = 2.65, p-value = 0.024), and 40–60 cm and 60–80 cm (z-statistic = 2.80, p-value = 0.021; Table 6). For the samples collected from 1 mm from the terminal growth band, the only significant difference is between 20 and 40 cm and 80–100 cm (z-statistic = 2.88, p-value = 0.020; Table 7). In this case, the samples from those shells harvested deeper in the water column had a mean of 0.17‰ less than those shells from higher in the water.

4.3. $\delta^{13}C$ variation with depth

We conducted similar statistical analyses of $\delta^{13}C$, values for which were obtained from the same samples tested for $\delta^{18}O$ (Tables 3–5). When looking at the 0–3 mm profile values, there is minimal variability in $\delta^{13}C$ (Fig. 5a; Table 3). The K-W test results corroborate this observation, as there are no significant differences among groups between these average carbon profile values (X^2 = 12.351, df = 9, p-value = 0.1942; Table 4). The differences in depth for individual shell measurements return similar results (Fig. 5b). As with oxygen, the data are variable, particularly at greater depths. When aggregating all of the individual point data and comparing for the corresponding points on each shell, there is a slight decrease in $\delta^{13}C$ with depth. The K-W test suggests there are statistically significant differences among depth levels (X^2 = 32.214, df = 9, p-value = 0.0002) and the post-hoc Dunn's Test shows only a significant difference between the middle and bottom depths (50–60 cm. – 90–100 cm., z-statistic = 3.90, p-value = 0.002; Table 5). The overall consistency through the water column indicates that depth is not an important factor influencing carbonate $\delta^{13}C$. Moreover, the $\delta^{13}C$ at 90–100 cm is only 0.20‰ less than 0–10 cm. The results indicate that there are large amounts of variability in $\delta^{13}C$, and any differences in this value with depth are relatively small. Similarly, when combining data from shells into 20 cm vertical levels, there are no significant differences in $\delta^{13}C$ with depth for any of the pairwise comparisons for either 0 mm or 1 mm from the terminal growth band of the shells (Fig. 5c; Tables 6 and 7).

5. Discussion

Length and stable oxygen isotopic measurements of *M. californianus* shells from Bechers Pier on Santa Rosa Island indicate significant differences with depth. Using the piling from a pier as a sampling location allows us to isolate a single spatial variable influencing these values, the vertical position in the water column. This is largely related to the amount of time the individual mussel spends submerged and exposed over the course of a tidal cycle. Those shells at the top of the mussel bed are exposed for greater amounts of time and consequently undergo frequent periods in which growth is slowed or even interrupted (Coe and Fox, 1942; Suchanek, 1981). This leads to smaller average lengths at the top of the bed and may be partially related to the differences in isotopic measurements because carbonate is only deposited in equilibrium with the surrounding water during part of the day. The base of the mussel growth range is typically constrained spatially by the presence of predators, who prevent colonization below the surf (Coe and Fox, 1942). In our case, this provides a distinct, one-meter thick test location.

The clearest differences with depth are in *M. californianus* shell length. There is a general increase in average shell size with depth from the top of the mussel bed to its peak from 50 to 70 cm, and then a smaller

Table 4
Adjusted p-values of pairwise comparisons from the Dunn's test for the 0–3 mm profile samples. $\delta^{18}O$ comparisons are below the diagonal and $\delta^{13}C$ comparisons are above.

Depth	0–10 cm	10–20 cm	20–30 cm	30–40 cm	40–50 cm	50–60 cm	60–70 cm	70–80 cm	80–90 cm	90–100 cm
0–10 cm	–	1	1	1	1	1	1	1	0.976	1
10–20 cm	0.683	–	1	1	1	1	1	1	1	1
20–30 cm	1	1	–	1	1	1	1	1	1	0.667
30–40 cm	1	1	1	–	1	1	1	0.495	1	0.098
40–50 cm	0.131	1	0.612	1	–	1	0.491	1	1	1
50–60 cm	0.557	1	1	1	1	–	1	1	1	0.612
60–70 cm	0.195	1	0.806	1	1	1	–	1	1	1
70–80 cm	0.138	1	0.613	1	0.492	1	1	–	1	1
80–90 cm	0.001*	0.626	0.021*	0.419	1	1	1	1	–	1
90–100 cm	0.108	1	0.549	1	0.945	1	1	1	1	–

* Values indicating a statistically significant difference at $\alpha = 0.05$ between depths

Table 5
Adjusted p-values of pairwise comparisons from the Dunn's test for all samples. $\delta^{18}O$ comparisons are below the diagonal and $\delta^{13}C$ comparisons are above.

Depth	0–10 cm	10–20 cm	20–30 cm	30–40 cm	40–50 cm	50–60 cm	60–70 cm	70–80 cm	80–90 cm	90–100 cm
0–10 cm	–	1	1	1	1	1	1	0.295	0.287	0.074
10–20 cm	0.634	–	1	1	0.499	1	1	0.239	0.239	0.051
20–30 cm	1	1	–	1	1	1	1	0.282	0.272	0.073
30–40 cm	0.489	1	1	–	0.949	1	1	0.275	0.279	0.072
40–50 cm	0.428	1	1	0.904	–	1	1	0.288	0.283	0.082
50–60 cm	0.275	1	0.843	1	1	–	0.276	0.015*	0.015*	0.002*
60–70 cm	0.003*	0.508	0.061	0.884	0.999	1	–	1	1	1
70–80 cm	0.0004*	0.191	0.014*	0.441	0.521	0.651	1	–	1	1
80–90 cm	0.000*	0.000*	0.000*	0.0001*	0.0002*	0.0004*	0.035*	0.239	–	1
90–100 cm	0.0004*	0.183	0.014*	0.43	0.513	0.651	1	0.49	0.248	–

* Values indicating a statistically significant difference at $\alpha = 0.05$ between depths.

decrease to the base. There is, however, greater variability in shell length with depth, with the maximum standard deviation occurring at those levels with the highest average length, between 50 and 80 cm in depth. This indicates that it is not simply that shells all get larger with depth, but that there is a potential for larger shells, with smaller ones also mixed in. This could potentially be because of crowding or higher growth rates. In addition to containing the largest shells, there also appears to be the highest density in these levels based on a visual assessment (Fig. 2). Furthermore, the increase in mussel size with depth is also visible in naturally occurring intertidal zones on Santa Rosa Island. In anecdotal observations, CSJ has noticed that the highest, most landward mussels within an intertidal bed tend to be the smallest on average, with an increase in size as one moves seaward and vertically downward. This trend was also observed in a study of mussel size by Thakar et al. (2017) on Santa Cruz Island. This pattern is characteristic of other similar species, making the most productive regions of the intertidal only accessible during more extreme low tides (e.g., Marean, 2014; Klein and Bird, 2016). In an archaeological context, therefore, this could exacerbate the differences between the uppermost and deeper mussels because the smaller shells of the upper intertidal may have been harvested more frequently and less able to have time to grow to larger sizes. This would not occur in our experimental location because shellfish harvesting is done there rarely, if ever.

Stable isotopic variation with depth is more germane to our central question, how the location of shells within the intertidal zone could alter our ability to accurately reconstruct past environmental conditions, including SST or patterns of upwelling. $\delta^{18}O$ is the more frequently used of the two measurements and it had a larger effect in this experiment. Overall, there is a small decrease in $\delta^{18}O$ values with depth. Because SST and $\delta^{18}O$ are negatively correlated (e.g., Epstein et al., 1953; Horibe and Oba, 1972), sampling a shell from the base of the vertical range would lead to warmer water temperature estimates on average than a shell from the top. When comparing the aggregated measurements for the different depths, the deepest shells were 0.42‰ less than the highest ones on average. Based on experimental measurements of seawater $\delta^{18}O$ for a four-year span from August 2015 to May 2019, annual variation is typically between −0.3‰ and −0.6‰, with an average of −0.4‰ and a standard deviation of 0.1‰ (Table 1). Therefore, while small, the effects of depth are larger than those of annual changes in the ambient seawater. Nevertheless, even changes in $\delta^{18}O$ resulting from depth are smaller than the annual fluctuation in SST. For example, using Eq. (1) and the average ambient $\delta^{18}O$ value for water of −0.4‰, a shell with a $\delta^{18}O$ value of 0‰ would yield a temperature estimate of 15.3 °C and a shell with a $\delta^{18}O$ value of −0.42‰ would yield a temperature estimate of 17.1 °C. This difference of 1.8 °C represents the extreme case of the difference between the top and bottom of the mussel bed and this potential error should be considered when attempting to reconstruct SST change through time. When only taking into account those samples from the edge of the shell, and therefore eliminating the risk that the results may be skewed by differential growth rates, the data indicate shells from lower in the water column were as much as 0.26‰ less than the highest ones on average. This supports the contention that the difference in SST estimates is likely less than the value of 1.8 °C. The bias in $\delta^{18}O$ associated with depth is difficult to quantify and these values represent different ways to estimate it using the same data set, although it is relatively small in both cases. Furthermore, it is likely that many shells grew in the middle of the intertidal, and not from the very top or bottom of the growth range, in which case there could be an error associated with depth that is less than this estimated value.

Differences between $\delta^{13}C$ measurements at the top and bottom of the mussel bed are smaller than those for $\delta^{18}O$. There were no significant differences in $\delta^{13}C$ measurements for the 0–3 mm profile sample or any of the individual sampled locations on the shell. When all point samples were considered together, there were no patterns between different levels of the mussel colony. While there is a statistically significant difference in $\delta^{13}C$ for a small number of specific locations in the mussel bed, there is also large variability between shells. Therefore, depth is unlikely to influence $\delta^{13}C$ measurements on archaeological shells when they are used to reconstruct long-term environmental change.

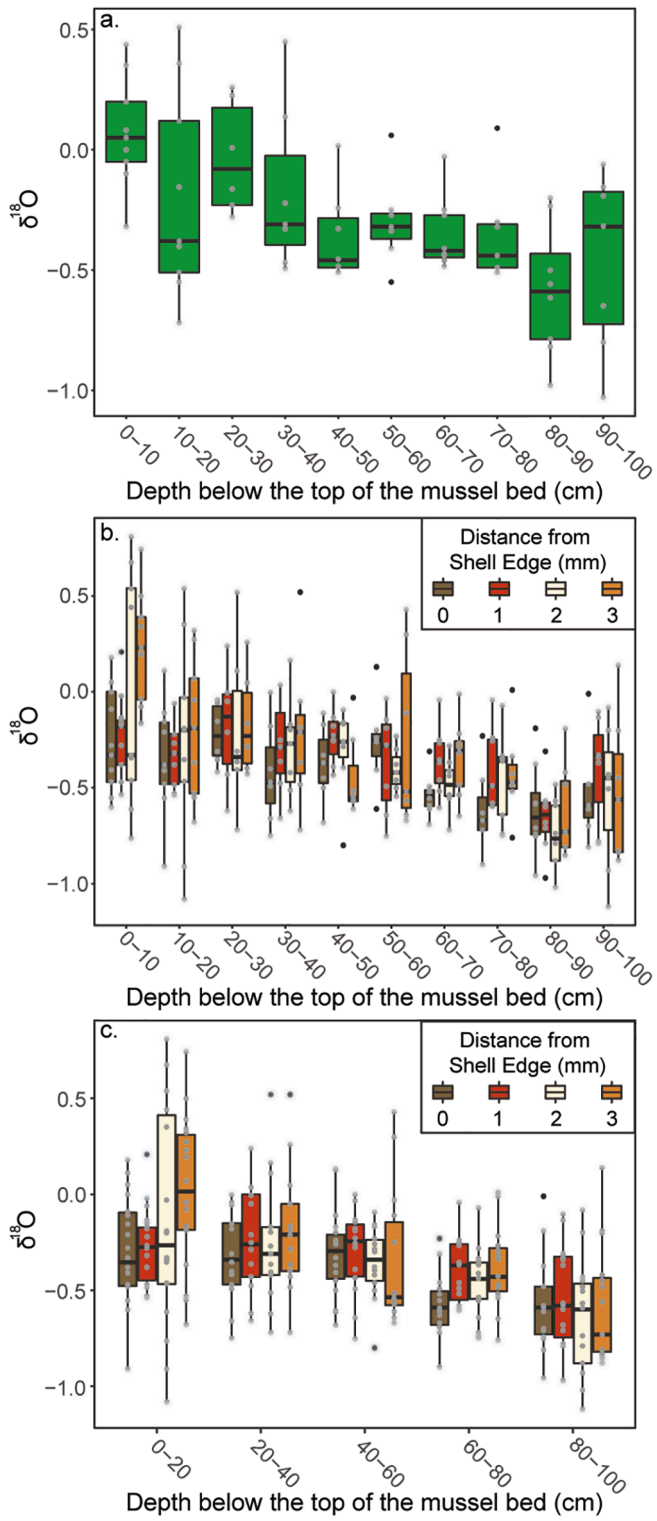

Fig. 4. $\delta^{18}O$ values by depth. (a) 0–3 mm profile samples; and (b) samples collected 0, 1, 2, and 3 mm from the outer edge/terminal growth band individually. The shaded portion makes up the interquartile range of the data between the upper and lower quartiles (25th-75th percentiles). The horizontal bar represents the median at each depth. The tails represent the minimum and maximum. Gray dots represent individual measurements and black dots represent possible outliers.

Table 6
Adjusted p-values of pairwise comparisons from the Dunn's test for samples taken 0 mm from the edge of each shell, aggregated into 20 mm levels. $\delta^{18}O$ comparisons are below the diagonal and $\delta^{13}C$ comparisons are above.

Depth	0–20 cm	20–40 cm	40–60 cm	60–80 cm	80–100 cm
0–20 cm	–	0.413	0.87	0.083	0.245
20–40 cm	1.000	–	0.766	0.074	0.258
40–60 cm	1.000	0.926	–	0.033	0.137
60–80 cm	0.009*	0.024*	0.021*	–	1.000
80–100 cm	0.009*	0.021*	0.019*	0.493	–

* Values indicating a statistically signifcant difference at $\alpha = 0.05$.
Note: Due to the adjustment for family-wise error rate, we reject H_0 if $p <= \alpha/2$.

Table 7
Adjusted p-values of pairwise comparisons from the Dunn's test for samples taken 1 mm from the edge of each shell, aggregated into 20 mm levels. $\delta^{18}O$ comparisons are below the diagonal and $\delta^{13}C$ comparisons are above.

Depth	0–20 cm	20–40 cm	40–60 cm	60–80 cm	80–100 cm
0–20 cm	–	0.461	0.659	0.782	0.129
20–40 cm	0.942	–	0.538	0.955	0.148
40–60 cm	0.469	0.7003	–	0.440	0.028
60–80 cm	0.542	0.485	0.665	–	0.626
80–100 cm	0.04	0.020*	0.043	0.438	–

* Values indicating a statistically significant difference at $\alpha = 0.05$.
Note: Due to the adjustment for family-wise error rate, we reject H_0 if $p <= \alpha/2$.

5.1. Implications for archaeology

Archaeologists frequently use $\delta^{18}O$ measurements of carbonate from *M. californianus* shells recovered from coastal midden sites for two primary reasons: (1) to assess changes in SST throughout human occupation of the region; and (2) to estimate the seasons during which people harvested mussels at the site. The latter has implications for understanding the seasons of site occupation and patterns of subsistence and mobility. Unfortunately, it is not possible to determine from where in the intertidal zone a particular mussel from an archaeological site was harvested. Shell length would be an unreliable indicator largely because of variability throughout the water column. Additionally, mussels from archaeological contexts could be influenced by human overpredation, which could cause a decrease in average size over time (e.g., Jones and Richman, 1995; Bettinger et al., 1997; Braje et al., 2007). Furthermore, frequent harvesting from a particular mussel bed without overpredation could lead to a decrease in mussel density, which could also increase average size because of a lack of overcrowding.

In the effort to reconstruct diachronic changes in SST, the effects of the vertical position of a mussel in the water column can be addressed in two ways. First is to recognize the inherent error that could be as much as 0.42‰ and potentially 1.8 °C. The second is to test multiple shells from a single context. While that increases the cost, it also increases the likelihood that shells from different vertical positions are sampled, thus potentially mitigating this source of error. In the second goal, to estimate seasons of mussel harvesting, we are aided in two ways. First, as described above, even at its greatest magnitude, the difference in $\delta^{18}O$ between samples from the top and bottom of the mussel bed is less than the annual cycle associated with seasonal water temperature changes. Second is the fact that mussels are sessile and do not move once they have attached to a location in the intertidal zone. Because the effects of depth would then be consistent throughout the year, it should still be possible to observe cyclical patterns in $\delta^{18}O$ and therefore estimated SST along the growth band of the shell. Therefore, the entire annual sinusoidal curve should be shifted, rather than just individual points. Drilling multiple samples per shell rather than one or two should better allow for the determination of season of harvest of that mussel, as long as it does not rely on measurements from other shells that may or may not have grown at the same depth.

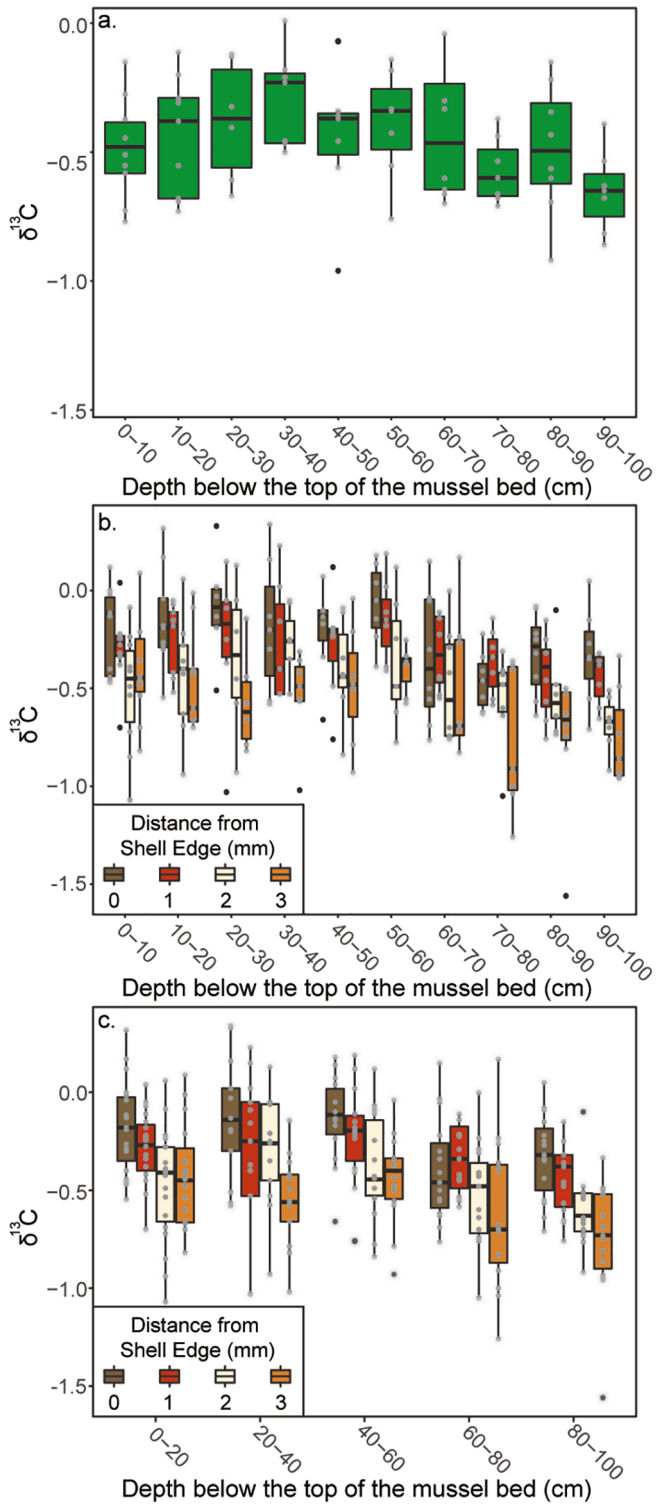

Fig. 5. $\delta^{13}C$ values by depth. (a) 0–3 mm profile samples; and (b) samples collected 0, 1, 2, and 3 mm from the outer edge/terminal growth band individually. The box plot is as in Fig. 4.

6. Conclusion

This study was a simple experiment to assess the effects of growing depth within the water column for *M. californianus* shells on average shell length, $\delta^{18}O$, and $\delta^{13}C$. By testing modern shells from distinct strata on a piling from a pier in a location with minimal harvesting by people, we were able to isolate the relationship between this single spatial variable and measurements of interest for paleoclimatology and archaeology. There was a clear relationship between depth and average mussel length, with the smallest individuals at the top of the mussel bed and a general increase in size down to a maximum between 50 and 70 cm below the top. This would not be unexpected to anyone who has spent time in an intertidal zone and has undoubtedly observed larger individuals at greater depths. The decrease with depth in $\delta^{18}O$ is statistically significant and should be taken into account with larger uncertainties when reconstructing changes in annual SST ranges through time. It also provides further support that season of harvest estimates for mollusk shells benefit from measuring enough samples to observe multiple seasons within the annual SST curve and not rely on annual ranges derived from other shells, which may or may not have grown at the same depth in the water column. This study contributes to a growing body of literature on refining methods for using marine mollusks from archaeological sites for paleoenvironmental reconstructions and estimates of site seasonality. Along with other studies, it will increase the usefulness of these techniques for understanding past environmental conditions and human-environment dynamics.

CRediT authorship contribution statement

Christopher S. Jazwa: Conceptualization, Methodology, Formal analysis, Investigation, Resources, Writing - original draft, Writing - review & editing, Visualization, Funding acquisition. **Christopher A. Wolfe:** Formal analysis, Writing - original draft, Writing - review & editing. **Elaine Y. Chu:** Formal analysis, Writing - review & editing. **Kyra E. Stull:** Methodology, Formal analysis, Writing - review & editing.

Acknowledgments

We would like to thank Channel Island National Park, including Kelly Minas, Laura Kirn, Kristin Hoppa, Lulis Cuevas, and Drew Adams for assistance with this project. The project was supported by the National Science Foundation (BCS-1724639, Jazwa) and the University of Nevada, Reno. We would like to thank Cause Hanna (January 2016) and Geoff Dilly (January 2018) for their assistance collecting water samples. Kevin Smith assisted with shell collection in August 2017 and Andrea Sbei, Samuel Jantz, Scarlett Boling, Carolina Juarez, Kaitlyn McKenna, and Zachary Khan helped with drilling shells. We appreciate the assistance of Sebastian Breitenbach with the isotopic measurements and sample analysis. Thank you also to Chris O. Hunt, Niklas Hausmann, and an anonymous reviewer for valuable comments and suggestions on drafts of this manuscript.

References

Andrus, C.F.T., 2011. Shell midden sclerochronology. Quat. Sci. Rev. 30, 2892–2905.
Andrus, C.F.T., Crowe, D.E., 2002. Alteration of otolith aragonite: effects of prehistoric cooking methods on otolith chemistry. Archaeol. Sci. 29, 291–299.
Bettinger, R.L., Malhi, R., McCarthy, H., 1997. Central place models of acorn and mussel processing. J. Archaeol. Sci. 24, 887–899.
Braje, T.J., Kennett, D.J., Erlandson, J.M., Culleton, B.J., 2007. Human impacts on nearshore shellfish taxa: a 7,000 year record from Santa Rosa Island, California. Am. Antiquity 72 (4), 735–756.
Branscombe, T.L., Bosch, M.D., Miracle, P.T., 2020. Seasonal shellfishing across the east Adriatic Mesolithic-Neolithic transition: oxygen isotope analysis of *Phorcus turbinatus* from Vela Spila (Croatia). Environ. Archaeol. https://doi.org/10.1080/14614103.2020.1721695.
Breitenbach, S.F.M., Bernasconi, S.M., 2011. Carbon and oxygen isotope analysis of small carbonate samples (20 to 100 μg) with a GasBench II preparation device. Rapid Commun. Mass Spectrom. 25, 1910–1914.
Butler, P.G., Schöne, B.R., 2017. New research in the methods and applications of sclerochronology. Palaeogeogr. Palaeoclimatol. Palaeoecol. 465, 295–299.
Butler, P.G., Wanamaker, A.D., Scourse, J.D., Richardson, C.A., Reynolds, D.J., 2013. Variability of marine climate on the North Icelandic Shelf in a 1357-year proxy archive based on growth increments in the bivalve Arctica Islandica. Palaeogeogr. Palaeoclimatol. Palaeoecol. 373, 141–151.

Button, K., Ioannidis, J., Mokrysz, C., Nosek, B.A., Flint, J., Robinson, E.S.J., Munafò, M. R., 2013. Power failure: why small sample size undermines the reliability of neuroscience. Nat. Rev. Neurosci. 14, 365–376.
Coe, W.R., Fox, D.L., 1942. Biology of the California sea-mussel (*Mytilus californianus*). I. influence of temperature, food supply, sex and age on the rage of growth. J. Experim. Biol. 90 (1), 1–30.
Coe, W.R., Fox, D.L., 1944. Biology of the California sea-mussel (*Mytilus californianus*). III. environmental conditions and rate of growth. Biol. Bull. 87, 59–72.
Colonese, A.C., Camaros, E., Verdun, E., Estevez, J., Giralt, S., Rejas, M., 2011. Integrated archaeozoological research of shell middens: new insights into hunter-gatherer-fisher coastal exploitation in Tierra del Fuego. J. Island Coast. Archaeol. 6 (2), 235–254.
Colquhoun, D., 2017. The reproducibility of research and the misinterpretation of p-values. R. Soc. Open Sci. 4, 171085.
Dinno, A., 2017. Dunn.test: Dunn's test of multiple comparisons using rank sums. R package version 1.3.5. https://CRAN.R-project.org/package=dunn.test.
Dodd, J.R., 1964. Environmentally controlled variation in the shell structure of a Pelecypod species. J. Paleontol. 38 (6), 1065–1071.
Dunn, O.J., 1964. Multiple comparisons using rank sums. Technometrics 6 (3), 241–252.
Eerkens, J.W., DeGeorgey, A., Spero, H.J., Descantes, C., 2014. Seasonality of late prehistoric clamming on San Francisco Bay: oxygen isotope analyses of *Macoma nasuta* Shells from a Stege Mound, CA-CCO-297. California Archaeol. 6 (1), 23–46.
Epstein, S., Buchsbaum, R., Lowenstam, H., Urey, H.C., 1953. Revised carbonate-water isotopic temperature scale. Bull. Geol. Soc. Am. 64, 1315–1326.
Flores, C., 2017. Importance of small-scale paleo-oceanographic conditions to interpret changes in size of California mussel (*Mytilus californianus*). Late Holocene, Santa Cruz island, California. Quatern. Int. 427, 137–150.
Glassow, M.A., Kennett, D.J., Kennett, J.P., Wilcoxon, L.R., 1994. Confirmation of middle Holocene ocean cooling inferred from stable isotopic analysis of prehistoric shells from Santa Cruz Island, California. In: Halvorson, W.L., Maender, G.J. (Eds.), The Fourth California Islands Symposium: Update on the Status of Resources. Santa Barbara Museum of Natural History, Santa Barbara, pp. 223–232.
Graniero, L.E., Surge, D., Gillikin, D.P., Briz i Godino, I., Álvarez, M., 2017. Assessing elemental ratios as a paleotemperature proxy in the calcite shells of patelloid limpets. Palaeogeogr. Palaeoclimatol. Palaeoecol. 465 (Part B), 376–385.
Gutiérrez-Zugasti, I., Suárez-Revilla, R., Clarke, L.J., Schöne, B.R., Bailey, G.N., González-Morales, M.R., 2017. Shell oxygen isotope values and sclerochronology of the limpet *Patella vulgata* Linnaeus 1758 from northern Iberia: implications for the reconstruction of past seawater temperatures. Palaeogeogr. Palaeoclimatol. Palaeoecol. 484, 48–61.
Harger, J.R.E., 1970. The effect of wave impact on some aspects of the biology of sea mussels. The Veliger. 12 (4), 401–414.
Hausmann, N., Colonese, A.C., de Lima Ponzoni, A., Hancock, Y., Meredith-Williams, M., Leng, M.J., Bailey, G.N., 2017. Isotopic composition of *Conomurex fasciatus* shells as an environmental proxy for the Red Sea. Quat. Int. 427, 115–127.
Holm, S., 1979. A simple sequentially rejective multiple test procedure. Scand. J. Stat. 6, 65–70.
Horibe, Y., Oba, T., 1972. Temperature scales of aragonite – water and calcite – water systems. Fossils. 23 (24), 69–79.
Jazwa, C.S., 2015. A Dynamic Ecological Model for Human Settlement on California's Northern Channel Islands. Ph.D. dissertation. Pennsylvania State University, University Park.
Jazwa, C.S., Braje, T.J., Erlandson, J.M., Kennett, D.J., 2015. Central place foraging and shellfish processing on California's northern Channel Islands. J. Anthropol. Archaeol. 40, 33–47.
Jazwa, C.S., Jantz, S., 2019. The effects of heating on $\delta^{18}O$ and $\delta^{13}C$ in *Mytilus californianus* shell carbonate: implications for paleoenvironmental reconstruction and season of harvest. J. California Great Basin Anthropol. 39 (2), 163–177.
Jazwa, C.S., Joslin, T.L., Kennett, D.J., 2020. Fishing, subsistence change, and foraging strategies on western Santa Rosa Island, California. American Antiquity. doi: 10.1017/aaq.2020.18.
Jazwa, C.S., Kennett, D.J., Winterhalder, B., 2016. A test of ideal free distribution predictions using targeted survey and excavation on California's northern Channel Islands. J. Archaeol. Method Theory 23, 1242–1284.
Jazwa, C.S., Kennett, D.J., Hanson, D., 2012. Late Holocene subsistence change and marine productivity on western Santa Rosa Island, California. California Archaeol. 4 (1), 69–97.
Jew, N.P., Erlandson, J.M., Watts, J., White, F.J., 2013. Shellfish, seasonality, and stable isotope sampling: $\delta^{18}O$ analysis of mussel shells from an 8,800-year-old shell midden on California's Channel Islands. J. Island Coastal Archaeol. 8, 170–189.
Jew, N.P., Erlandson, J.M., Rick, T.C., Reeder-Myers, L., 2014. Oxygen isotope analysis of California mussel shells: seasonality and human sedentism at an 8,200-year-old shell midden on Santa Rosa Island, California. Archaeol. Anthropol. Sci. 6 (3), 293–303.
Jones, T.L., Richman, J.R., 1995. On mussels: *Mytilus californianus* as a prehistoric resource. North Am. Archaeol. 16 (1), 33–58.
Kennett, D.J., 1998. Behavioral Ecology and the Evolution of Hunter-Gatherer Societies on the Northern Channel Islands, California. Ph.D. dissertation. University of California, Santa Barbara.
Kennett, D.J., Voorhies, B., 1996. Oxygen isotopic analysis of archaeological shells to detect seasonal use of wetlands on the southern Pacific Coast of Mexico. J. Archaeol. Sci. 23, 689–704.
Klein, R.G., Bird, D., 2016. Shellfishing and human evolution. J. Anthropol. Archaeol. 44, 198–205.
Kruskal, W.H., Wallis, W.A., 1952. Use of ranks in one-criterion variance analysis. J. Am. Stat. Assoc. 47 (260), 583–621.
Loftus, E., Lee-Thorp, J., Leng, M., Marean, C., Sealy, J., 2019. Seasonal scheduling of shellfish collection in the Middle and Later Stone Ages of southern Africa. J. Hum. Evol. 128, 1–6.
Marean, C., 2014. The origins and significance of coastal resource use in Africa and western Europe. J. Hum. Evol. 77, 17–40.
Milano, S., Prendergast, A.L., Schöne, B.R., 2016. Effects of cooking on mollusk shell structure and chemistry: implications for archaeology and paleoenvironmental reconstruction. J. Archaeolog. Sci.: Rep. 7, 14–26.
Müller, P., Staudigel, P.T., Murray, S.P., Vernet, R., Barusseau, J., Westphal, H., Swart, P. K., 2017. Prehistoric cooking versus accurate palaeotemperature records in shell midden constituents. Nature Sci. Rep. 7 (3555), 1–11.
Paine, R.T., 1976. Biological observations on a subtidal *Mytilus californianus* bed. Veliger 19, 125–130.
Parker, W.G., Yanes, Y., Surge, D., Mesa-Hernández, E., 2017. Calibration of the oxygen isotope ratios of the gastropods *Patella candei crenata* and *Phorcus atratus* as high-resolution paleothermometers from the subtropical eastern Atlantic Ocean. Palaeogeogr. Palaeoclimatol. Palaeoecol. 487, 251–259.
Prendergast, A.L., Schöne, B.R., 2017. Oxygen isotopes from limpet shells: Implications for palaeothermometry and seasonal shellfish foraging studies in the Mediterranean. Palaeogeogr. Palaeoclimatol. Palaeoecol. 484, 33–47.
Prendergast, A.L., Pryor, A.J.E., Reade, H., Stevens, R.E., 2018. Seasonal records of palaeoenvironmental change and resource use from archaeological assemblages. J. Archaeolog. Sci.: Rep. 21, 1191–1197.
R Core Team., 2018. R: A language and environment for statistical computing. R Foundation for Statistical Computing, Vienna, Austria https://www.R-project.org/.
Sadler, J., Carré, M., Azzoug, M., Schauer, A.J., Ledesma, J., Cardenas, F., Chase, B.M., Bentaleb, I., Muller, S.D., Mandeng, M., Rohling, E.J., Sachs, J.P., 2012. Reconstructing past upwelling intensity and the seasonal dynamics of primary productivity along the Peruvian coastline from mollusk shell stable isotopes. Geochem. Geophys. Geosyst. 13 (1), 1–17.
Shackleton, N.J., 1973. Oxygen isotope analysis as a means of determining season of occupation of prehistoric midden sites. Archaeometry. 15 (1), 133–141.
Soot-Ryen, T., 1955. A report on the family Mytilidae (Pelecypoda). Allan Hancock Pacific Expeditions. 20, 1–174.
Suchanek, T.H., 1978. The ecology of *Mytilus edulis* L. in exposed rocky intertidal communities. J. Exp. Mar. Biol. Ecol. 31, 105–120.
Suchanek, T.H., 1981. The role of disturbance in the evolution of life history strategies in the intertidal mussels Mytilus edulis and Mytilus californianus. 50, 143-152.
Thakar, H.B., 2014. Food and Fertility in Prehistoric California: A Case-Study of Risk-Reducing Foraging Behavior and Prehistoric Population Growth from Santa Cruz Island, California. Ph.D. dissertation. University of California, Santa Barbara.
Thakar, H.B., Glassow, M.A., Blanchette, C., 2017. Reconsidering evidence of human impacts: implications of within-site variation of growth rates in *Mytilus californianus* along tidal gradients. Quat. Int. 427, 151–159.
Thomas, K.D., 2015. Molluscs emergent, Part I: themes and trends in the scientific investigation of mollusc shells as resources for archaeological research. J. Archaeol. Sci. 56, 133–140.
Thompson, V.D., Andrus, C.F.T., 2011. Evaluating mobility, monumentality, and feasting at the Sapelo Island shell ring complex. Am. Antiq. 76 (2), 315–343.
Urey, H.C., 1947. The thermodynamic properties of isotopic substances. J. Chem. Soc. 1947, 562–581.
Wefer, G., Berger, W.H., 1987. Isotope paleontology: growth and composition of extant calcareous species. Mar. Geol. 100, 207–248.
West, C.F., Burchell, M., Andrus, C.F.T., 2018. Molluscs and paleoenvironmental reconstruction in Island and coastal settings: variability, seasonality, and sampling. In: Giovas, C.M., LeFebvre, M.J. (Eds.), Zooarchaeology in Practice: Case Studies in Methodology and Interpretation in Archaeofaunal Analysis. Springer, New York, pp. 191–208.
Wickham, H., 2016. Ggplot2: Elegant Graphics for Data Analysis. Springer-Verlag, New York.